IEEE Access
Multidisciplinary | Rapid Review | Open Access Journal

Received January 12, 2018, accepted March 7, 2018, date of publication March 19, 2018, date of current version April 18, 2018.

Digital Object Identifier 10.1109/ACCESS.2018.2817023

False-Positive Reduction on Lung Nodules Detection in Chest Radiographs by Ensemble of Convolutional Neural Networks

CHAOFENG LI[1], (Member, IEEE), GUOCE ZHU[2], XIAOJUN WU[2], (Member, IEEE), AND YUANQUAN WANG[3]

[1]Institute of Logistics Science and Engineering, Shanghai Maritime University, Shanghai 200135, China
[2]School of Internet of Things Engineering, Jiangnan University, Wuxi 214122, China
[3]School of Computer Science, Hebei University of Technology, Tianjin 300401, China

Corresponding author: Chaofeng Li (wxlichaofeng@126.com)

This work was supported in part by the National Natural Science Foundation of China under Grant61771223, in part by NSF of Hebei Province through the Key Program under Grant F2016202144, and in part by the Department of Education of Hebei Province through the Youth Fund under Grant QN2016217.

ABSTRACT Aiming at the problem that traditional lung nodules detection method can only get low sensitivities with a lot of false positives, we propose a new framework of ensemble of convolutional neural networks (E-CNNs) and use it to significantly reduce the number of false positive on lung nodules detection in chest radiographs (CXRs). First, unsharp mask technique is used to enhance the nodules in the CXRs. Then, we cut patches in the 229 × 229 image containing or not containing nodule from the enhanced CXRs, which correspond to the positive and negative samples. Third, three optimized CNNs of different input sizes and different depths, namely, CNN1, CNN2 and CNN3, are constructed to detect lung nodule separately, and their input sizes are 12 × 12, 32 × 32, and 60 × 60, and the number of layers are 5, 7, and 9, separately. Finally, a logical AND operator is used to fuse the results of CNN1, CNN2, and CNN3, and E-CNNs are constructed for detecting lung nodules. Our experimental results on the Japanese Society of Radiological Technology database show our proposed E-CNNs attain a sensitivity of 94% and 84% with an average of 5.0 false-positives (FPs) per image and 2.0 FPs per image, respectively, in a five-fold cross-validation test, which far outperforms the state of the art.

INDEX TERMS Chest radiographs (CXRs), lung nodules detection, convolutional neural network (CNN), ensemble learning.

I. INTRODUCTION

Lung cancer is about 14% of all new cancer diagnoses in 2016. The 5-year relative survival rate for lung cancer is only 17% [1]. Early detection and treatment of lung cancers are very important as the 5-year survival rate can increase up to 55% if the tumor is detected accurately and diagnosed early.

The detection of lung nodules in chest radiographs (CXRs) becomes a major diagnostic problem, as the clinical detection of lung cancer is mainly carried out by identifying lung nodules. There are two kinds of chest imaging techniques, basic X-ray imaging and computed tomography (CT). The CT is considered to be the most effective imaging method for detecting lung nodules at an early stage. However, CT is expensive and often not available in low-level hospitals. In contrast, the basic chest radiographs are the most cost-effective, dose-effective and routinely available diagnostic tool, so CXRs is the first diagnostic step for detecting any chest abnormalities. Improvements in the detection of lung nodules in CXRs could have a significant impact on early detection of lung cancer.

Superimposed anatomical structures make the image complicated. Interpreting a chest radiograph is not an easy thing. Even experienced radiologists have trouble distinguishing infiltrates from the normal pattern of branching blood vessels in the lung fields, or detecting subtle nodules that indicate lung cancer. With the importance of CXRs and their complicated nature, it is necessary for developing

computer algorithms to assist radiologists in reading CXRs.

It has been a long time for the study of computer-aided diagnosis (CAD) system of lung nodule detection, which has been explored to make the identification of lung nodules quicker and more accurate. Mastsumoto *et al*. [2] show that it cannot help the doctors to improve diagnostic accuracy, even though CAD system gets the sensitivity over 80% at the false-positives (FPs) per image level of 11. When the FPs is reduced to 4.0, the CAD system can be useful for the doctors. The biggest challenge of current CAD system is how to reduce the FP over a high level of sensitivity. Keserci and Yoshida [3] use edge guided wavelet snake model to extract the edge of rib and nodule edge coverage feature, and then reduce the false positive rate by using this feature and other morphological features. Yoshida [4] use the removal of the rib structure based on the left and right lung area symmetry to reduce false positives. Penedo *et al*. [5] present a two-level artificial neural network architecture to enhance lung nodules in CXRs. Suzuki *et al*. [6] developed a multi-resolution massive training artificial neural network image processing technique that helps suppress the contrast of ribs and clavicles in CXRs. Chen *et al*. [7] use a two-stage enhancement technology to improve the sensitivity. Chen and Suzuki [8] use ''virtual dual-energy'' technique to improve the sensitivity. Chen *et al*. [9] developed a parameterized logarithmic image processing method to enhance lung nodules in chest radiographs. Though in recent 10 years the performance of detecting lung nodules is increased a lot, there remain many false-positives needed to be reduced.

In recent 5 years, with the rapid development of deep learning, convolutional neural network (CNN) has made big progress, especially in image classification and object detection. The advantage of CNN is that it can extract features automatically by using large amounts of data to obtain better result. Weight sharing and back-propagation (BP) algorithm can help the model get a better generalization performance and global optimal [10]–[12].

In this paper, we propose a new method of ensemble of convolutional neural networks (E-CNNs) to directly detect lung nodules, which omits the lung field segmentation procedure, and avoids the loss of true lung nodules of traditional detection scheme [13] when extracting the lung field.

The remainder of this paper is organized as follows. In section 2, Image dataset, CNN models and our proposed E-CNNs for detection of lung nodules are introduced. Experimental results and analysis are made in Section 3. We discuss and conclude in Section 4 and Section 5, respectively.

II. MATERIALS AND METHODS

A. IMAGE DATASET

The database provided by Japanese Society of Radiological Technology (JSRT) [14] is used. The CXRs in the database were collected from 14 medical institutions by using screen-film systems over a period of 3 years. All nodules in the CXRs were confirmed by CT, and the locations of the nodules were confirmed by three chest radiologists who were in complete agreement. The images were digitized to yield 12-bit CXRs with a resolution of 2048 × 2048 pixels. The size of pixel was 0.175 × 0.175mm. The original JSRT database contained 93 normal cases, which were defined that there were not any nodule and diseases in these CXRs, and 154 cases with confirmed lung nodules. The cases with confirmed lung nodules were grouped into 5 categories based on the subtlety of detection. For simplicity, we re-divide the nodules into two classes for the experiments: 'practicable' for obvious, relatively obvious, subtle cases, and 'hard' for very subtle and extremely subtle cases, as listed in Table 1.

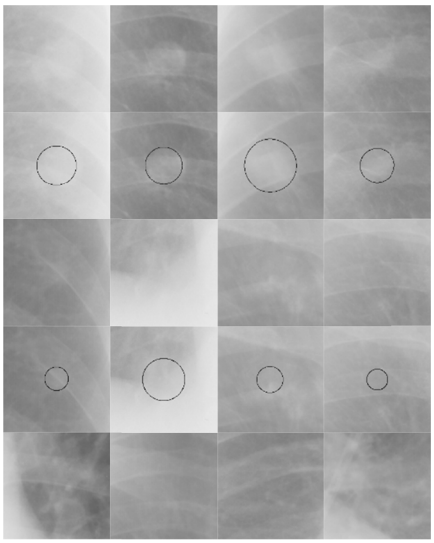

FIGURE 1. Some nodule and non-nodule patches. First row is practicable group, and the second row is ground truth of first row, and the third row is hard group, and the fourth row is the ground truth of third row, and the last row is non-nodule patches.

Here we display some nodule and non-nodule patches in Fig.1, which the circles demonstrate the location and the size of the nodules given by the JSRT. It can be found that nodules and non-nodules are very difficult to be distinguished if without the ground truth, especially for hard group.

B. CNN FOR LUNG NODULES DETECTION

The whole procedure of CNN for detecting lung nodules is shown in Fig.2. Firstly the nodule signals are enhanced, then we subsample the patches cut from the enhanced CXRs with slide-window method, and feed into the CNN model to detect lung nodules.

1) IMAGE PREPROCESSING

In this paper, we use Unsharp Mask (USM) [15] image sharpening technique to enhance the nodule signal in the CXRs. The equation is as follows:

$$I_s = I_o + (I_o - I_b) * Amount \tag{1}$$

TABLE 1. The distribution of lung nodules in the JSRT.

	size			total
	Small	Medium	Large	
Extremely subtle	2	18	5	25(16.2%)
Very subtle	3	16	10	29(18.8%)
Subtle	4	29	17	50(32.5%)
Relatively obvious	1	20	17	38(24.7%)
Obvious	0	5	7	12(7.8%)
hard	**5**	**34**	**15**	**54(35.1%)**
practicable	**5**	**54**	**41**	**100(64.9%)**

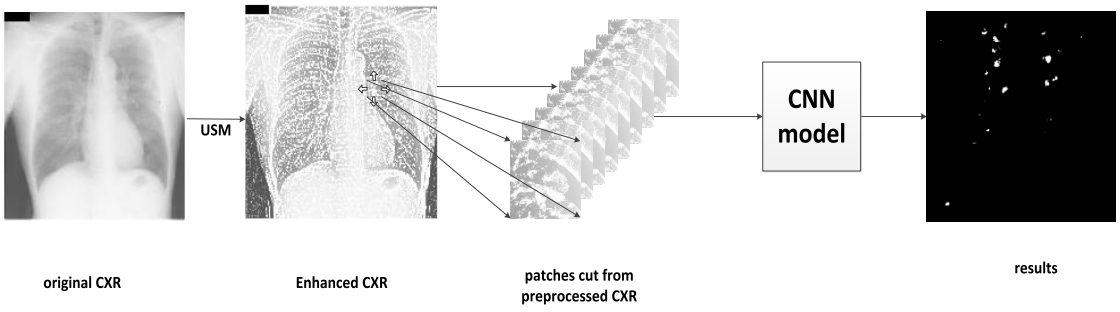

FIGURE 2. The procedure of Lung nodules detection using CNN.

where $\boldsymbol{I_s}$ denotes the sharpened image, and $\boldsymbol{I_o}$ is the original image, and $\boldsymbol{I_b}$ is the blurred image, and *Amount* denotes how much contrast is added at the edges. Here, we use Gaussian Blur technique to blur image, and set *Amount* to 50.

As shown in Fig.3, the circle denotes the location of the true nodule. It can be seen that the nodule in Fig.3(b) is much more obvious than the original one in Fig.3(a).

2) CONSTRUCTING ARCHITECTURE OF CNN

The CNN is a highly nonlinear filter that can be trained by using input images and the corresponding teaching labels. It always consists of multi convolutional layers, pooling layers and fully connected layers. Our constructed basic architecture of CNN for detecting lung nodules is shown in Fig.4, which the input images are the 32×32 patches cut from the enhanced CXRs.

3) CONVOLUTIONAL LAYER AND POOLING LAYER

The convolutional layer extracts images features using convolutional calculation with different convolutional kernels. Each kernel convolves the input to output a kind of feature. This configuration simulates the local perception characteristics of human visual system. In this computation, activation function is very important. Rectified Linear Units (ReLUs) [16] is wide used as activation function in the newly proposed CNN models. Study from Krizhevsky *et al*. [17] demonstrated that ReLUs enable the network to train several times faster than

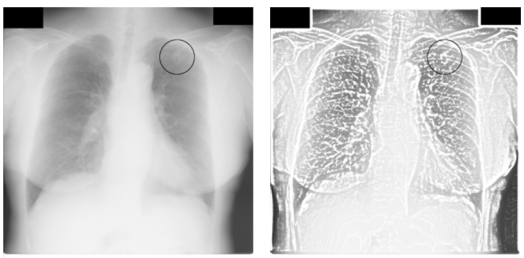

FIGURE 3. (a) original CXR JPCLN030, (b) enhanced CXR of JPCLN030.

using tanh units in deep CNN. The equation is as following.

$$f(x) = \max(0, \sum_i w_i a_i) \tag{2}$$

where $\boldsymbol{w}$ is the connection weights, and α is the output from the formal layer.

In this paper, we use linear activation function in the first and second convolutional layers, and ReLUs function in the third convolutional layer and the last fully connected layer.

4) TRAINING

We train our network from scratch on patches taken from large images. By taking small patches as input, much larger number of training samples are gained, which meet the needs of CNNs. For training the whole model, the loss function is

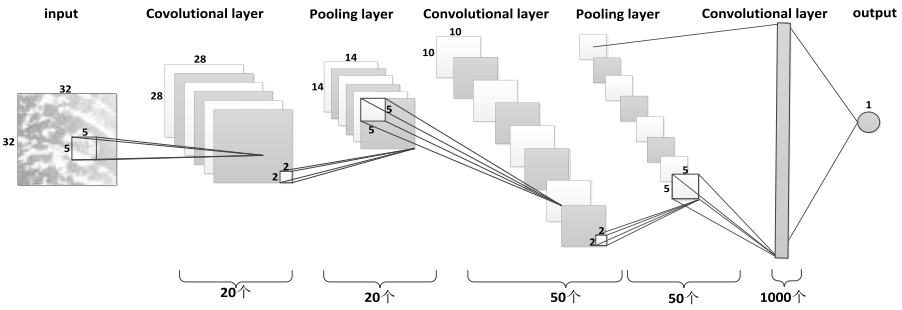

FIGURE 4. The architecture of CNN for lung nodules detection.

defined as follows:

$$L = \frac{1}{2} \|f(w; x) - y\|^2 \tag{3}$$

where $\boldsymbol{x}$ is the input patch, and $\boldsymbol{w}$ are weights for each layer, and f is the candidate predict function. $\boldsymbol{y}$ denotes whether the input patch contains a true lung nodule, and 1 for yes, and 0 for no. The back-propagation and stochastic gradient descent (SGD) methods are used to train the weights as follows:

$$w' = \min_{w} L \tag{4}$$

$$\Delta w = \nabla_w L \tag{5}$$

$$w = w + \alpha \Delta w \tag{6}$$

C. ENSEMBLE OF CNNs (E-CNNs) FOR LUNG NODULES DETECTION

1) ALGORITHM INTRODUCTION

The similarities to different scales of patches are different. As shown in Fig.5, even if it is subsampled from the original patches, and can still be recognized as containing nodules. But those similar to the subsampled patches known as false-positives are different. So in this paper, we propose an ensemble model of CNNs to reduce false positives.

One single CNN has limited learning capacity, and may not learn all the essential features to distinguish a nodule from various types of non-nodule structure, but multi different CNNs can deal with much more non-nodules. So we propose the Ensemble of CNNs (E-CNNs) to reduce the false-positives.

Different Architectures of CNN can deal with different input images. With different scales of subsample of the patches, our proposed E-CNNs model deal with the non-nodule patch differently. When they all can mark the true positive (TP), we can reduce the false positives by a complete agreement.

2) ARCHITECTURE of E-CNNs

Here we construct 3 CNNs for different input scales, i.e. CNN1, CNN2 and CNN3, and their architectures shown in Table 2. The architecture of proposed E-CNNs is shown in Fig.6, and a logical AND operator is used to fuse the results

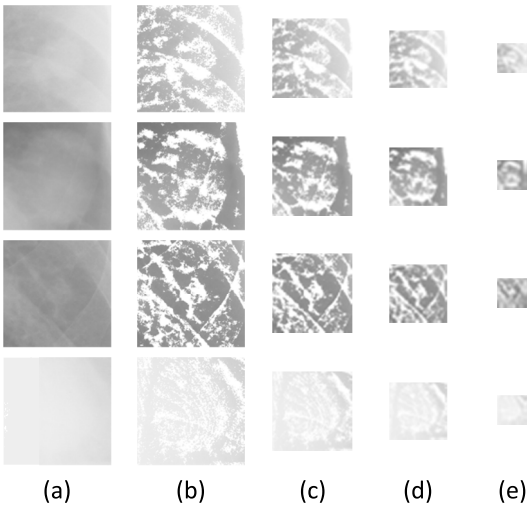

FIGURE 5. Nodule patches of different scales. (a) the raw patches, (b) the USM enhanced patches, (c) 60 × 60 patches, (d) 32 × 32 patches, (e) 12 × 12 patches.

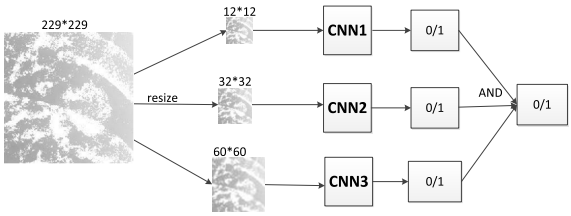

FIGURE 6. The architecture of the ensemble of CNNs.

of CNN1, CNN2 and CNN3. An example of results of using different CNN is shown in Fig.7, which demonstrates lots of false-positives are reduced by using the E-CNNs compared Fig.7(a), (b), (c) with Fig.7 (d).

III. EXPERIMENTAL RESULTS AND ANALYSIS

In this section, the 5-fold cross validation test method and free-response receiver operating characteristic (FROC) [18] were applied for analyzing the performance of nodule detection. To evaluate the performance, the true positive standard needs to be defined. In the JSRT, the nodule size ranged from 5 to 60mm with an average size of 24.6mm. With reference

TABLE 2. The CNN architectures used in our experiments.

Layer	Type	Input	Kernel	Stride	Pad	Output
(a) CNN1						
0	Input	12×12	N/A	N/A	N/A	12×12
1	Convolution	12×12	5×5	1	0	20×8×8
2	Max pooling	20×8×8	2×2	2	0	20×4×4
3	Convolution	20×4×4	4×4	1	0	1000×1
4	Fully Connected	1000×1	1×1	1	0	1×1
(b) CNN2						
0	input	32×32	N/A	N/A	N/A	32×32
1	Convolution	32×32	5×5	1	0	20×28×28
2	Max pooling	20×28×28	2×2	2	0	20×14×14
3	Convolution	20×14×14	5×5	1	0	50×10×10
4	Max Pooling	50×10×10	2×2	2	0	50×5×5
5	Convolution	50×5×5	5×5	1	0	1000×1
6	Fully Connected	1000×1	1×1	1	0	1×1
(c) CNN3						
0	input	60×60	N/A	N/A	N/A	60×60
1	Convolution	60×60	5×5	1	0	20×56×56
2	Max pooling	20×56×56	2×2	2	0	20×28×28
3	Convolution	20×28×28	5×5	1	0	50×24×24
4	Max pooling	50×24×24	2×2	2	0	50×12×12
5	Convolution	50×12×12	5×5	1	0	100×8×8
6	Max pooling	100×8×8	2×2	2	0	100×4×4
7	Convolution	100×4×4	4×4	1	0	1000×1
8	Fully Connected	1000×1	1×1	1	0	1×1

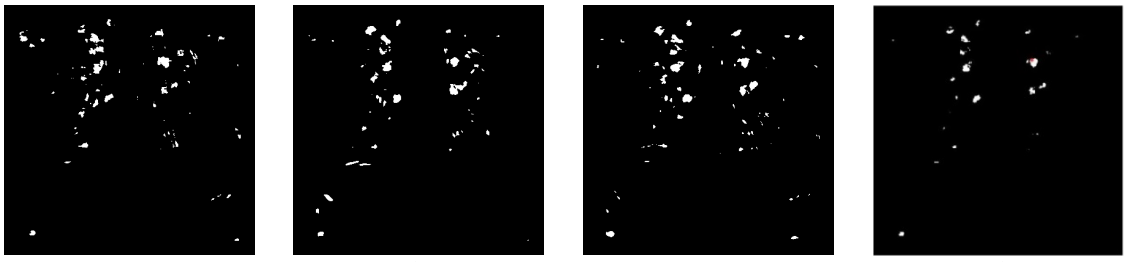

FIGURE 7. Results of JPCLN030 using CNN, (a) Results of CNN1; (b) Results of CNN2; (c) Results of CNN3; (d) Results of E-CNNs. The red dot in (d) denotes the true nodule location.

to [19]–[22], we use distance criterion of smaller than 25mm as the true positive standard.

A. PERFORMANCE FOR DIFFERENT SUBTLETY

Here FROC curve are used to show the performance of the system in the JSRT database, as in Fig.8. It can be seen that our proposed method achieves a sensitivity of 94% with an average of 5.0 FPs per image, and 96% for the practicable group, and 92% for the hard group. Schilham *et al*. [23] show that for the hard group only 44% from radiologists, which suggests our method outperforms the radiologists, which is encouraging for practical use.

B. PERFORMANCE COMPARISON BETWEEN SINGLE CNN AND E-CNNs

FROC curves of using single CNN and E-CNNs are shown in Fig.9. It can be seen E-CNNs achieves a sensitivity of 84% while the other three single CNN can only get 57% at the average FPs of 2.0, which demonstrates that the E-CNNs outperforms the single CNN1, CNN2 and CNN3 considerably.

C. PERFORMANCE COMPARISON BETWEEN E-CNNs AND FINETUNED ALEXNET

Alexnet [17] is well known in deep learning framework, and here we compare our proposed E-CNNs with it. We replace

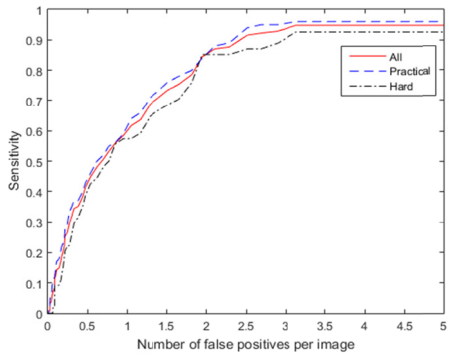

FIGURE 8. Performance of E-CNNs for different subtlety of nodules in the JSRT.

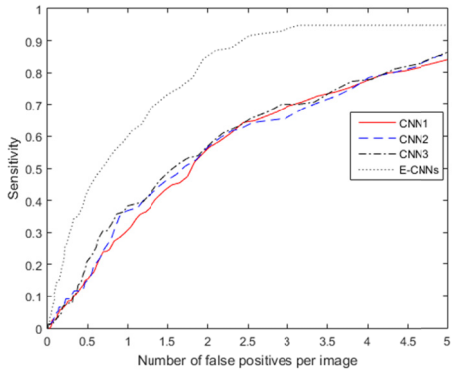

FIGURE 9. Performance comparison between E-CNNs and CNN1, CNN2, CNN3.

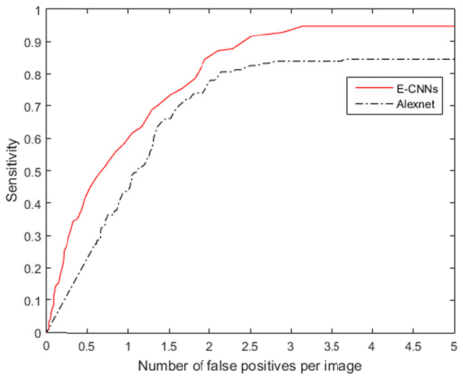

FIGURE 10. Performance comparison between E-CNNs and Alexnet.

the Softmax layer with a one node output regression layer, and trained the AlexNet with the same training set as above.

The performances are shown in Fig.10. It can be seen that the E-CNNs outperforms the Alexnet in all cases.

Due to the large scale of the input and the complexity of architecture of Alexnet, it is hard to be run in ordinary computer. Here we also compare their patch process time as shown in Fig.11. The test software environment is Win10 and Matlab2015a, and the hardware environment is CPU of Intel i7, 16G memory and GTX960m of GPU. It can be that Alexnet costs much more time than CNN1, CNN2, CNN3 and E-CNNs. As the calculation of each CNN of E-CNNs can go

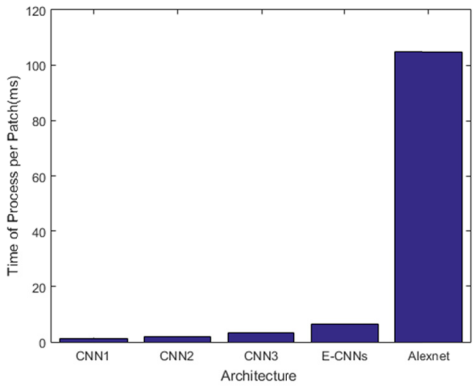

FIGURE 11. Time cost comparison among our proposed CNNs and Alexnet.

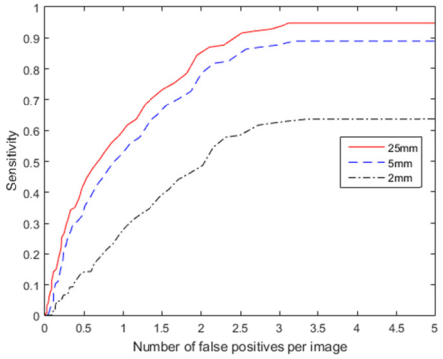

FIGURE 12. Performances of different distance criterion for determining TP detections.

parallel, the time of E-CNNs spent can just be a little higher than single CNN3. So our proposed E-CNNs outperforms the Alexnet for lung nodule detection both in accuracy and efficiency.

D. PERFORMANCE FOR TWO STANDARDS OF TRUE POSITIVE

The performance differs a lot with different standards for true positive. Performances of three different distance criterion are shown in Fig.12. It can be seen that it is effective even the distance criterion is set to 5mm which is shorter than the diameter of all the nodules in the JSRT.

IV. DISCUSSIONS

Due to different database, different TP criteria, and different evaluation procedures, it is hard to make definitive comparisons with previously published CAD scheme, so we compare the performance reported in the literature in the JSRT database. Wei *et al*. reported that their CAD scheme achieved a sensitivity of 80% with 5.4 FPs per image for the JSRT database [24]. Hardie *et al*. [19] reported that their scheme marked 80% of nodules in the subset of the JSRT database with 5 FPs per image. Their performance was calculated by use of the ''distance'' criterion of 25mm for determining TP detections. As shown in the Table 3, our proposed E-CNNs can achieve a sensitivity of 94% with 5.0 FPs per image, and

TABLE 3. Performance comparisons of CAD schemes in the JSRT database.

Methods		Sensitivity	FPs/image	Database
Wei et al.(2002) [24]		80%(123/154)	5.4(1333/247)	All CXRs in JSRT
Coppini et al.(2003) [25]		60%(93/154)	4.3(662/154)	All CXRs with nodule in JSRT
Schiham et al.(2006)[23]		51%(79/154)	2.0(308/154)	ALL CXRs with nodule in JSRT
		67%(103/154)	4.0(616/154)	
Hardie et al.(2008)[19]		80%(112/140)	5.0(700/140)	140 CXRs with nodule in JSRT
		63%(88/140)	2.0(280/140)	
Chen et al.	Two-stage nodule enhancement(2011) [7]	71.4%(110/154)	5.0(1235/247)	140 CXRs with nodule and non-nodule CXRs in JSRT
		64.9%(100/154)	2.0(494/247)	
	VDE-based CADe(2013) [8]	85%(119/140)	5.0(1165/233)	
Proposed CNN2		**86%(133/154)**	5.0(1235/247)	ALL CXRs in JSRT
		57%(89/154)	2.1(503/247)	
Proposed Ensemble CNNs		**94%(146/154)**	4.6(1131/247)	
		84%(130/154)	2.0(480/247)	

83% with 2.0 FPs per image for all nodules in the JSRT, which far outperforms the current reported methods. The current reported best result is only 85% (119/140) with 5.0 FPs from [8], and moreover 14 true lung nodules are lost in [8].

V. CONCLUSIONS

In this paper, we have developed three CNN Frameworks and an E-CNNs model for detecting lung nodules in CXRs. Our E-CNNs scheme achieve sensitivity of 84% (130/154), and 94% (146/154) with 2.0 (480/247) FPs/image, and 4.6 (1131/247) FPs/image in the JSRT database in 5-fold cross validation test, and achieves a sensitivity of 92% with 5.0 FPs/image for the hard group which is encouraging for practical use.

REFERENCES

[1] *American Cancer Society. Cancer Facts & Figures 2016*, Amer. Cancer Soc., Atlanta, GA, USA, 2016.
[2] T. Matsumoto *et al.*, "Image feature analysis of false-positive diagnoses produced by automated detection of lung nodules," *Investigative Radiol.*, vol. 27, no. 8, pp. 587–597, 1992.
[3] B. Keserci and H. Yoshida, "Computerized detection of pulmonary nodules in chest radiographs based on morphological features and wavelet snake model," *Med. Image Anal.*, vol. 6, no. 4, pp. 431–447, 2002.
[4] H. Yoshida, "Local contralateral subtraction based on bilateral symmetry of lung for reduction of false positives in computerized detection of pulmonary nodules," *IEEE Trans. Biomed. Eng.*, vol. 51, no. 5, pp. 778–789, May 2004.
[5] M. G. Penedo, M. J. Carreira, A. Mosquera, and D. Cabello, "Computer-aided diagnosis: A neural-network-based approach to lung nodule detection," *IEEE Trans. Med. Imag.*, vol. 17, no. 6, pp. 872–880, Dec. 1998.
[6] K. Suzuki, H. Abe, H. MacMahon, and K. Doi, "Image-processing technique for suppressing ribs in chest radiographs by means of massive training artificial neural network (MTANN)," *IEEE Trans. Med. Imag.*, vol. 25, no. 4, pp. 406–416, Apr. 2006.
[7] S. Chen, K. Suzuki, and H. MacMahon, "Development and evaluation of a computer-aided diagnostic scheme for lung nodule detection in chest radiographs by means of two-stage nodule enhancement with support vector classification," *Med. Phys.*, vol. 38, no. 4, pp. 1844–1858, 2011.
[8] S. Chen and K. Suzuki, "Computerized detection of lung nodules by means of 'virtual dual-energy' radiography," *IEEE Trans. Biomed. Eng.*, vol. 60, no. 2, pp. 369–378, Feb. 2013.
[9] S. Chen, L. Yao, and B. Chen, "A parameterized logarithmic image processing method with Laplacian of Gaussian filtering for lung nodule enhancement in chest radiographs," *Med. Biol. Eng. Comput.*, vol. 54, no. 11, pp. 1793–1806, 2016.
[10] Y. LeCun, L. Bottou, Y. Bengio, and P. Haffner, "Gradient-based learning applied to document recognition," *Proc. IEEE*, vol. 86, no. 11, pp. 2278–2324, Nov. 1998.
[11] R. Girshick, J. Donahue, T. Darrell, and J. Malik, "Region-based convolutional networks for accurate object detection and segmentation," *IEEE Trans. Pattern Anal. Mach. Intell.*, vol. 38, no. 1, pp. 142–158, Jan. 2016.
[12] X.-J. Zhang, Y.-F. Lu, and S.-H. Zhang, "Multi-task learning for food identification and analysis with deep convolutional neural networks," *J. Comput. Sci. Technol.*, vol. 31, no. 3, pp. 489–500, 2016.
[13] B. Van Ginneken, B. M. Ter Haar Romeny, and M. A. Viergever, "Computer-aided diagnosis in chest radiography: A survey," *IEEE Trans. Med. Imag.*, vol. 20, no. 12, pp. 1228–1241, Dec. 2001.
[14] J. Shiraishi *et al.*, "Development of a digital image database for chest radiographs with and without a lung nodule: Receiver operating characteristic analysis of radiologists' detection of pulmonary nodules," *Amer. J. Roentgenol.*, vol. 174, no. 1, pp. 71–74, 2000.
[15] A. Polesel, G. Ramponi, and V. J. Mathews, "Image enhancement via adaptive unsharp masking," *IEEE Trans. Image Process.*, vol. 9, no. 3, pp. 505–510, Mar. 2000.
[16] V. Nair and G. E. Hinton, "Rectified linear units improve restricted Boltzmann machines," in *Proc. 27th Int. Conf. Mach. Learn. (ICML)*, 2010, pp. 1–8.
[17] A. Krizhevsky, I. Sutskever, and G. E. Hinton, "Imagenet classification with deep convolutional neural networks," in *Proc. Adv. Neural Inf. Process. Syst.*, 2012, pp. 1097–1105.
[18] J. P. Egan, G. Z. Greenberg, and A. I. Schulman, "Operating characteristics, signal detectability, and the method of free response," *J. Acoust. Soc. Amer.*, vol. 33, no. 8, pp. 993–1007, 1961.

[19] R. C. Hardie, S. K. Rogers, T. Wilson, and A. Rogers, "Performance analysis of a new computer aided detection system for identifying lung nodules on chest radiographs," *Med. Image Anal.*, vol. 12, no. 3, pp. 240–258, 2008.
[20] J. Shiraishi, Q. Li, K. Suzuki, and R. Engelmann, "Computer-aided diagnostic scheme for the detection of lung nodules on chest radiographs: Localized search method based on anatomical classification," *Med. Phys.*, vol. 33, no. 7, pp. 2642–2653, 2006.
[21] C. Sheng and L. Li, "A new computer aided diagnostic scheme for lung nodule detection on chest radiograph," *Acta Electron. Sin.*, vol. 38, no. 5, pp. 1211–1216, 2010
[22] C. Bao *et al.*, "Computer-assisted detection of lung nodules based on virtual dual energy subtraction soft-tissue radiograph generation technology," *Chin. J. Med. Imag. Technol.*, vol. 31, no. 8, pp. 1276–1280, 2015.
[23] A. M. R. Schilham, B. van Ginneken, and M. Loog, "A computer-aided diagnosis system for detection of lung nodules in chest radiographs with an evaluation on a public database," *Med. Image Anal.*, vol. 10, no. 2, pp. 247–258, 2006.
[24] J. Wei *et al.*, "Optimal image feature set for detecting lung nodules on chest X-ray images," in *Computer Assisted Radiology and Surgery*. Berlin, Germany: Springer, 2002, pp. 706–711.
[25] G. Coppini, S. Diciotti, M. Falchini, N. Villari, and G. Valli, "Neural networks for computer-aided diagnosis: Detection of lung nodules in chest radiograms," *IEEE Trans. Inf. Technol. Biomed.*, vol. 7, no. 4, pp. 344–357, Dec. 2003.

CHAOFENG LI received the B.S. and M.S. degrees in mathematical geology and the Ph.D. degree in remote sensing image processing from the China University of Mining and Technology, Xuzhou, China, in 1995, 1998, and 2001, respectively. From 2001 to 2003, he was Post-Doctoral Researcher in pattern recognition and intelligent systems with the Nanjing University of Science and Technology. He was a Visiting Research Scholar with the University of Texas at Austin from 2008 to 2009. He is currently a Professor with the Logistics Research Center, Shanghai Maritime University. He is an Associate Professor and a Professor with the School of Internet of Things Engineering, Jiangnan University, from 2003 to 2017.

He has published over 80 papers in reputable journals and conference proceedings, covering the areas of neural network, image processing, and analysis. His current research interests include image processing, machine learning, and medical image analysis.

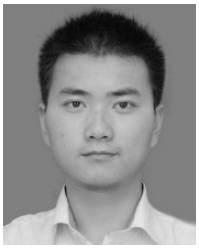

GUOCE ZHU was born in Taizhou, Jiangsu, China, in 1990. He received the B.S. degree in computer science and technology from the Taihu University of Wuxi in 2012 and the M.S. degree from Jiangnan University in 2017. His current research interests include medical image processing, machine learning, deep learning and its applications.

XIAOJUN WU received the B.Sc. degree in mathematics from Nanjing Normal University, Nanjing, China, in 1991, and the M.S. degree in computer science and the Ph.D. degree in pattern recognition and intelligent systems from the Nanjing University of Science and Technology, Nanjing, in 1996 and 2002, respectively.

He is currently a Professor of artificial intelligent and pattern recognition with Jiangnan University, Wuxi, China. His current research interests include pattern recognition, computer vision, fuzzy systems, neural networks, and intelligent systems.

YUANQUAN WANG received the master's and Ph.D. degree from the Nanjing University of Science and Technology (NUST) in 1998 and 2004, respectively. From 1998 to 2001, he was a software engineer in industry. In 2004, he held a Post-Doctoral Position with the Beijing Institute of Technology. He is currently a Professor of computer science and software engineering with the Hebei University of Technology. He received the Most Outstanding Postgraduate Award from NUST in 1998.

He has published dozens of papers in reputable journals and conference proceedings, covering the areas of computer vision, image processing, and medical image analysis. His current research interests include intelligent analysis of cardiac MRI and MRA, development of technologies to transfer research concepts into tools for clinical study, image and video captioning, and VQA-based on deep learning.